Entanglement dynamics of a three-qubit system with different interatomic distances*

Feng Ling-Juan(封玲娟)[a], Zhang Ying-Jie(张英杰)[a)b)], Zhang Lu(张 路)[a], and Xia Yun-Jie(夏云杰)[a)†]

[a] *Shandong Provincial Key Laboratory of Laser Polarization and Information Technology, Department of Physics, Qufu Normal University, Qufu* 273165, *China*

[b] *Beijing National Laboratory of Condensed Matter Physics, Institute of Physics, Chinese Academy of Sciences, Beijing* 100190, *China*

(Received 25 April 2015; revised manuscript received 17 June 2015; published online 9 October 2015)

We investigate the tripartite entanglement dynamics of three two-level atoms in a multi-mode vacuum field. By considering the influences of the interatomic distance and the initial condition on the lower bound of concurrence and the tripartite negativity, we show that an optimal interatomic distance can be found to minimize the collective damping. Interestingly, at the same optimal distance, the tripartite entanglement would be maximized in the open dynamics process. In the case of shorter interatomic distance, the tripartite entanglement can display the oscillatory behavior in the initial short-time limit and be trapped in a stationary value in the long-time limit. In addition, the tripartite entanglement for the general situation with different interatomic distances is also discussed.

Keywords: quantum entanglement, the lower bound of concurrence, W state, interatomic distance

PACS: 03.67.–a, 03.65.Yz, 03.65.Ud **DOI:** 10.1088/1674-1056/24/11/110305

1. Introduction

In recent years, quantum entanglement, which plays a very important role in quantum information processing, has attracted extensive attention. However, due to the inevitable interaction of a realistic system with its surrounding environments, the entanglement degrades with time and even completely disappears in a finite time, which is termed as the entanglement sudden death.[1–4] Therefore, it is important to protect entanglement as a major resource for quantum information and quantum computation.

So far, there has been much literature on the dynamics of a bipartite atomic system under different kinds of environments including independent and common ones.[5–9] It is observed that in the non-Markovian reservoirs, the entanglement sudden birth appearing after complete disappearance depends on the initial state of the system.[10,11] Besides, in the thermal and vacuum environments, taking into account the two atoms close together, due to the presence of collective damping and dipole–dipole interaction, Tahira *et al.*[12–16] found the revival of entanglement and the oscillatory behavior. In the same model, Berrada *et al.*[17] studied the quantum correlation of each atom with its environment in terms of the critical distance. As is well known, the multipartite entanglement is significant for quantum tasks in many areas of physics, such as quantum information and communication theory.[18] Because of its complexity and lack of good measures, many aspects of the multipartite entanglement are not well studied. Recently, the dynamics of three qubits was investigated with the dipole–dipole interactions and the atom–cavity couplings considered.[19–24] An *et al.*[25] proposed a model of three atoms coupled to a common environment and investigated the tripartite entanglement via the lower bound of concurrence.

In this paper, we investigate the entanglement dynamics of a three-qubit atomic system interacting with a multimode vacuum field. When the atoms are initially prepared in W-like states and arranged in two different geometries (an equilateral triangle and a line), we study the influences of the distance between the atoms and the initial condition on the tripartite entanglement by using the lower bound of concurrence and the tripartite negativity.[26–28] Considering the equality of all the pairwise distances, we can obtain the analytical result via the Laplace transform. For the initially entangled states, the optimal interatomic distance that minimizes the collective damping is exactly the one that maximizes the tripartite entanglement. While for some initially separable states, this is not the case. In the short time limit, we can see the oscillatory (or exponential) behavior of the tripartite entanglement at very small (or large) distances. In the long time limit, the tripartite entanglement tends to a stationary value which is dependent on the interatomic distance and the initial condition. Moreover, contrary to the previous studies, we investigate the situation with different distances between the atoms. The paper is organized as follows. In Section 2, we present the model for our system, where the lower bound of concurrence and the tripartite nega-

*Project supported by the National Natural Science Foundation of China (Grant Nos. 61178012, 11204156, and 11304179), the Specialized Research Fund for the Doctoral Program of Higher Education, China (Grant Nos. 20133705110001 and 20123705120002), and the Natural Science Foundation of Shandong Province, China (Grant Nos. BS2013DX034, ZR2012FQ024, and ZR2014AP009).

†Corresponding author. E-mail: yjxia@mail.qfnu.edu.cn

© 2015 Chinese Physical Society and IOP Publishing Ltd

tivity play important parts in the measure of the three-qubit entanglement. In Section 3, we study some important factors like the interatomic distance and different initial conditions which can influence the entanglement in the tripartite system. In Section 4, we summarize our work. In the Appendix, we obtain the exact solutions for W states.

2. The model

We consider a quantum system in which three identical two-level atoms are coupled to a quantized multimode electromagnetic field. The atoms are close to each other, the transition dipole moment, the collective damping, and the dipole–dipole interaction cannot be ignored. In the interaction picture, the Hamiltonian of the system can be written as ($\hbar = 1$)

$$\begin{aligned} H &= -\mathrm{i}\sum_{i=1}^{3}\sum_{\boldsymbol{k}s}\left[\boldsymbol{d}_i\cdot\boldsymbol{g}_{\boldsymbol{k}s}(\boldsymbol{r}_i)a_{\boldsymbol{k}s}\sigma_i^{+}\,\mathrm{e}^{-\mathrm{i}(\omega_k-\omega_i)t}\right] \\ &\quad -\mathrm{i}\sum_{i=1}^{3}\sum_{\boldsymbol{k}s}\left[\boldsymbol{d}_i\cdot\boldsymbol{g}_{\boldsymbol{k}s}(\boldsymbol{r}_i)a_{\boldsymbol{k}s}\sigma_i^{-}\,\mathrm{e}^{-\mathrm{i}(\omega_k+\omega_i)t}\right]+\mathrm{H.c.}, \quad (1) \end{aligned}$$

where ω_i and ω_k are the transition frequency of the atoms and the frequency of the field mode, respectively; $\boldsymbol{d}_i$ is the atomic transition dipole moment; σ_i^{+} (σ_i^{-}) is the raising (lowering) operator of the i-th atom; and $a_{\boldsymbol{k}s}^{+}$ ($a_{\boldsymbol{k}s}$) is the creation (annihilation) operator of mode $\boldsymbol{k}s$ of the field with $\boldsymbol{k}$ the wave vector and s the index of polarization. The coupling constant can be given by

$$\boldsymbol{g}_{\boldsymbol{k}s}(\boldsymbol{r}_i)=\sqrt{\frac{\omega_k}{2\varepsilon_0 V}}\hat{\boldsymbol{e}}_{\boldsymbol{k}s}\exp\mathrm{i}\boldsymbol{k}\cdot\boldsymbol{r}_i, \quad (2)$$

where ε_0 is the vacuum permittivity, V is the quantization volume, $\hat{\boldsymbol{e}}_{\boldsymbol{k}s}$ is the electric field polarization vector, and $\boldsymbol{r}_i$ is the position of atom i.

According to the rotating wave approximation and a Markovian approximation, the Lehmberg–Agarwal master equation of the three atoms inside their local vacuum environments can be written as

$$\begin{aligned} \frac{\partial\rho}{\partial t} &= -\mathrm{i}\omega_0\sum_{i=1}^{3}[\sigma_i^z,\rho]-\mathrm{i}\sum_{i\neq j}^{3}\Omega_{ij}\left[\sigma_i^{+}\sigma_j^{-},\rho\right] \\ &\quad -\frac{1}{2}\sum_{i,j=1}^{3}\gamma_{ij}\left([\rho\sigma_i^{+},\sigma_j^{-}]+[\sigma_i^{+},\sigma_j^{-}\rho]\right), \quad (3) \end{aligned}$$

where $\sigma_i^z=\frac{1}{2}(|e\rangle_{ii}\langle e|-|g\rangle_{ii}\langle g|)$ is the i-th atom's energy operator, $|e\rangle_i$ ($|g\rangle_i$) is the excited (ground) state of the atoms, and $\gamma_{ij}\equiv\gamma\,(i=j)$ is the spontaneous decay rate. Moreover, γ_{ij} and Ω_{ij} $(i\neq j)$, depending on the distance between different atoms i and j, describe the collective damping and the dipole–dipole interaction, which can be respectively given by

$$\begin{aligned} \gamma_{ij} &= \frac{3}{2}\gamma(1-\cos^2\theta)\frac{\sin(kr_{ij})}{kr_{ij}} \\ &\quad +\frac{3}{2}\gamma(1-3\cos^2\theta)\left[\frac{\cos(kr_{ij})}{(kr_{ij})^2}-\frac{\sin(kr_{ij})}{(kr_{ij})^3}\right], \quad (4) \\ \Omega_{ij} &= -\frac{3}{4}\gamma(1-\cos^2\theta)\frac{\cos(kr_{ij})}{kr_{ij}} \\ &\quad +\frac{3}{4}\gamma(1-3\cos^2\theta)\left[\frac{\sin(kr_{ij})}{(kr_{ij})^2}+\frac{\cos(kr_{ij})}{(kr_{ij})^3}\right], \quad (5) \end{aligned}$$

where $k=2\pi/\lambda$, λ is the resonant wavelength of the atoms, $r_{ij}=|r_i-r_j|$ is the distance between the two atoms, and θ is the angle between the atomic transition dipole moments and the orientation of the interatomic axis. Furthermore, the results in the presence of collective damping and dipole–dipole interaction are complicated depending on different spatial configurations through the atomic transition dipole moment $\boldsymbol{d}_i$ and the interatomic distance r_{ij}. To account for this fact, we shall distinguish among three cases about the pairwise distances, that is, all the pairwise distances are equal ($r_{12}=r_{13}=r_{23}$, case 1); two of the three distances are equal but different from the third one ($r_{ij}=r_{kl}\neq r_{mn}$, case 2); all the pairwise distances are different ($r_{12}\neq r_{13}\neq r_{23}\neq r_{12}$, case 3).

Considering the initial state of the three-qubit atomic system[29] in the form

$$\begin{aligned} |\Psi\rangle &= \alpha_1|eee\rangle+\alpha_2|eeg\rangle+\alpha_3|ege\rangle+\alpha_4|gee\rangle \\ &\quad +\alpha_5|egg\rangle+\alpha_6|geg\rangle+\alpha_7|gge\rangle+\alpha_8|ggg\rangle, \quad (6) \end{aligned}$$

where α_i is the probability amplitude with the normalization condition $\sum_{i=1}^{8}\alpha_i^2=1$, we can obtain the solutions of the density matrix elements by solving the master equation (3) in the basis. Let $|1\rangle\to|eee\rangle$, $|2\rangle\to|eeg\rangle$, $|3\rangle\to|ege\rangle$, $|4\rangle\to|gee\rangle$, $|5\rangle\to|egg\rangle$, $|6\rangle\to|geg\rangle$, $|7\rangle\to|gge\rangle$, $|8\rangle\to|ggg\rangle$ for short.

In the following, we use two well-defined measures of the tripartite entanglement to assess the amount of entanglement analytically: the lower bound of concurrence and the tripartite negativity. First, for three qubits, we adopt the lower bound of concurrence as the measure of entanglement,[21,22,24–27] which is defined as

$$C_3=\sqrt{\frac{1}{3}\sum_{l=1}^{6}\left[\left(C_l^{12|3}\right)^2+\left(C_l^{13|2}\right)^2+\left(C_l^{23|1}\right)^2\right]}, \quad (7)$$

where $C_l^{ij|k}=\max\left\{0,\sqrt{\lambda_{l,1}^{ij|k}}-\sum_{q>1}\sqrt{\lambda_{l,q}^{ij|k}}\right\}$, $\lambda_{l,q}^{ij|k}$ are the eigenvalues listed in descending order of the matrix $\tilde{\rho}=\rho(L_l^{ij}\otimes\sigma_y^k)\rho^*(L_l^{ij}\otimes\sigma_y^k)$. Here, ρ^* is the complex conjugation of ρ in the basis of three qubits, L_l^{ij} is one of the six generators of group SO(4) operating on qubits i and j, and σ_y^k is the y Pauli matrix operating on qubit k.

Another entanglement is the tripartite negativity,[20,28] whose expression is given as

$$N_3=\left(N^{1-23}N^{2-13}N^{3-12}\right)^{1/3}, \quad (8)$$

where $N^{i-jk}=2\max\{0,-\lambda_{\min}\}$, $\lambda_{\min}$ are the lowest eigenvalues of the partially transposed matrix ρ^{T_i} of ρ

with respect to subsystem i, $\langle l_i,m_j,n_k|\rho^{T_i}|o_i,p_j,q_k\rangle = \langle o_i,m_j,n_k|\rho|l_i,p_j,q_k\rangle$ $(l,m,n,o,p,q=e,g)$.

3. Entanglement evolution

We suppose that the atoms are prepared in the W state at the initial time and emphasize that the choice of the present initial state is made only for clarity and the analysis is general. The W-like initial state is of the form

$$|\Psi\rangle = \alpha_5|egg\rangle + \alpha_6|geg\rangle + \alpha_7|gge\rangle. \tag{9}$$

Let us consider the situation of case 1 and $\theta = 5\pi/6$ which corresponds to the most symmetric configuration. That is to say, the atoms sit on the vertices of an equilateral triangle within the vacuum environment. Here, the nonzero solutions of the density matrix elements (see Appendix A) can be evaluated from the master equation (3) by means of the Laplace transform. Given the density matrix elements, we can now calculate the lower bound of concurrence and the tripartite negativity, which are respectively given by

$$C_3 = \sqrt{\frac{8}{3}(\rho_{55}\rho_{66}+\rho_{55}\rho_{77}+\rho_{66}\rho_{77})}, \tag{10}$$

$$\begin{aligned} N_3 = &-\left[\rho_{88}-\sqrt{4\rho_{55}(\rho_{66}+\rho_{77})+\rho_{88}^2}\right]^{1/3} \\ &\times\left[\rho_{88}-\sqrt{4\rho_{66}(\rho_{55}+\rho_{77})+\rho_{88}^2}\right]^{1/3} \\ &\times\left[\rho_{88}-\sqrt{4\rho_{77}(\rho_{55}+\rho_{66})+\rho_{88}^2}\right]^{1/3}. \end{aligned} \tag{11}$$

First, to explore the dependence of the dynamical behaviors of the tripartite entanglement on the interatomic distance, we plot, in the short time period, the lower bound of concurrence and the tripartite negativity as a function of the distance r_{12}/λ in Fig. 1. For the atoms that are initially prepared in the maximally entangled states ($\alpha_5=\alpha_6=\alpha_7=1/\sqrt{3}$), the explicit expressions of the lower bound of concurrence and the tripartite negativity can be respectively given as follows:

$$C_3 = \frac{2\sqrt{2}}{3}\sqrt{\mathrm{e}^{-2(2\gamma_{12}+\gamma)t}}, \tag{12}$$

$$\begin{aligned} N_3 = &\frac{1}{3}\sqrt{9+\mathrm{e}^{-2(2\gamma_{12}+\gamma)t}\left[17-18\,\mathrm{e}^{(2\gamma_{12}+\gamma)t}\right]} \\ &-1+\mathrm{e}^{-(2\gamma_{12}+\gamma)t}. \end{aligned} \tag{13}$$

From Eqs. (12) and (13), we can immediately conclude that C_3 and N_3 are primarily controlled through the collective damping, and are independent of the dipole–dipole interaction.

Figure 1 shows that the time evolutions of C_3 and N_3 behave similarly regarding the interatomic distance. Interestingly, during the same time period, there is one maximum of the entanglement at a specific distance, and we will discuss this in detail in the following. In Fig. 2(a), we show the variation of C_3 and N_3 with the distance for different values of the time γt. It is worth noticing that for each moment, at the optimal distance $r_{12}=0.814\lambda$, C_3 and N_3 reach their maximal values, and the entanglement of Fig. 1 also shows the slowest decay. At the same distance $r_{12}=0.814\lambda$, the collective damping $\gamma_{12}=-0.1079\gamma$ reaches its minimal value, as can be seen from Fig. 2(c). This indicates that the entanglement and the collective damping are very sensitive to the distance. Moreover, due to the spontaneous emission, for the same distance, C_3 and N_3 decrease monotonously down to zero with γt increasing in Fig. 1.

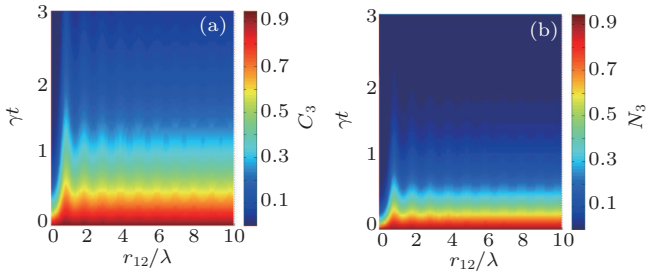


Fig. 1. (color online) Contour plots of two different measures of tripartite entanglement versus r_{12}/λ and γt with $\alpha_5=\alpha_6=\alpha_7=1/\sqrt{3}$: (a) C_3, (b) N_3.

However, comparing the two graphs of Fig. 1, we find that for the same distance, C_3 decays slower compared with N_3. To show this, we plot in Fig. 2(b) the time variation of the tripartite entanglement for different values of the collective damping γ_{12}. As observed from Fig. 2(b), γ_{12} increases from $\gamma_{12}=-0.1079\gamma$ up to $\gamma_{12}=\gamma$, which speeds up the atoms' disentangling process. Furthermore, it is clear by inspection of Eqs. (12) and (13) that for whatever γ_{12}, the death time of N_3 can be much longer than that of C_3.

Next, to highlight the distinct effect of the initial condition of the system on the entanglement among the three atoms, we plot, at a fixed moment of time ($\gamma t=1$), the difference of the entanglement with the interatomic distance r_{12}/λ for the initially entangled states from that of the initially separable states in Figs. 3(a) and 3(b). For the initially entangled states, the choice of the different values of the probabilities α_i does not alter the optimal distance for the maximal entanglement in comparison to some initially separable states. Moreover, in the situation of equal probabilities α_i (i.e., $\alpha_5=\alpha_6=\alpha_7$), the entanglement depends crucially on the collective damping, while in the situation of unequal probabilities α_i (i.e., $\alpha_i=\alpha_j\neq\alpha_k$ or $\alpha_i\neq\alpha_j\neq\alpha_k$), the entanglement is profoundly affected by the dipole–dipole interaction. From Figs. 2(a) and 3, we note also that when $r_{12}<0.37\lambda$, the dipole–dipole interaction can induce the oscillatory behavior of the entanglement. Meanwhile, due to the rapid energy exchange, the rapid oscillatory behavior of the entanglement happens at weak dipole–dipole

interaction. This fact explains the absence of the oscillatory behavior in Fig. 4(a) when $\alpha_5 = \alpha_6 = \alpha_7 = 1/\sqrt{3}$, as opposed to the presence of the oscillatory behavior in Fig. 4(b) when $\alpha_5 = 2/\sqrt{6}$ and $\alpha_6 = \alpha_7 = 1/\sqrt{6}$. Considering the non-existence of the dipole–dipole interaction and $r_{12} < 0.37\lambda$, the entanglement of Fig. 4(a) will quickly disappear in a finite time. On the contrary, the entanglement of Fig. 4(b) will tend to a stationary value in the long time limit. For shorter the atomic distance (i.e., $\gamma_{12} \approx \gamma$), from Eq. (10), the long-term behavior of the entanglement is derived as

$$C_3^{\infty}(t \to \infty) = \frac{2\sqrt{2}}{3\sqrt{3}}\left[1 - \alpha_6\alpha_7 - \alpha_5(\alpha_6 + \alpha_7)\right]. \quad (14)$$

From the above equation, it is obvious that the stationary value of the entanglement is not related to the concrete values of the collective damping and the dipole–dipole interaction. This result may accomplish protecting the entanglement for a sufficiently long time (i.e., it can slow down the degradation

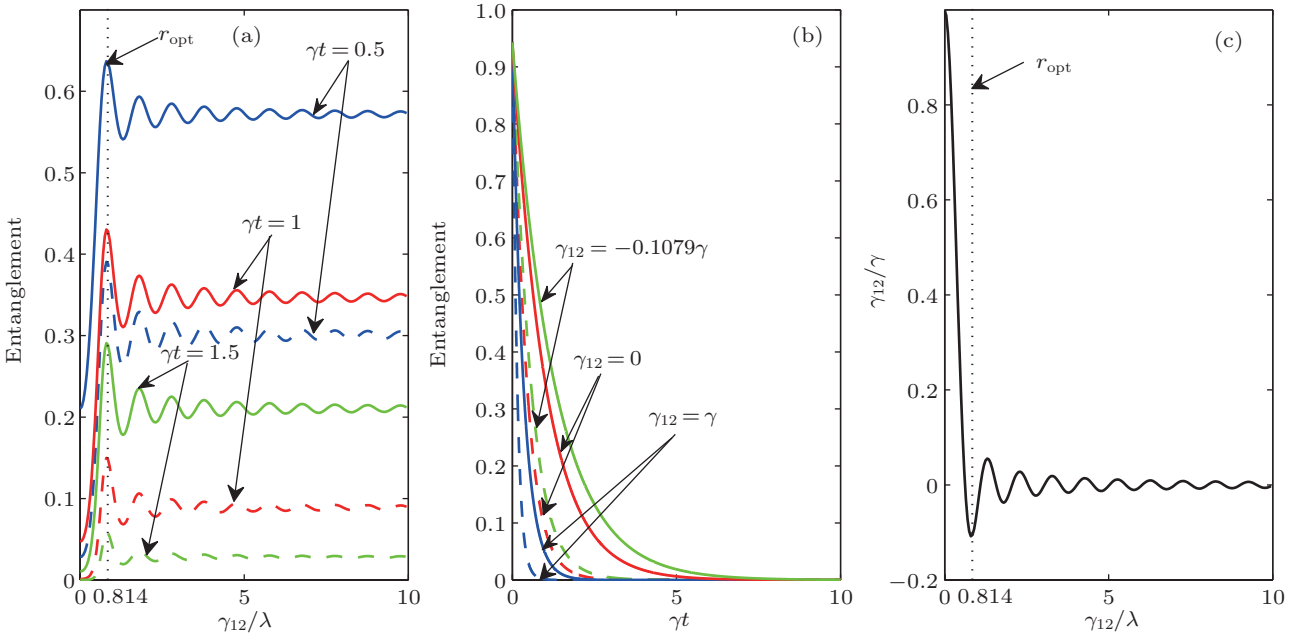


Fig. 2. (color online) (a) The entanglement versus r_{12}/λ with $\alpha_5 = \alpha_6 = \alpha_7 = 1/\sqrt{3}$ for various values of γt, and (b) the entanglement versus γt with $\alpha_5 = \alpha_6 = \alpha_7 = 1/\sqrt{3}$ for various values of γ_{12}.The solid (blue, red, green) line is for C_3, and the dashed (blue, red, green) line is for N_3. (c) The γ_{12}/γ versus r_{12}/λ with $\theta = 5\pi/6$.

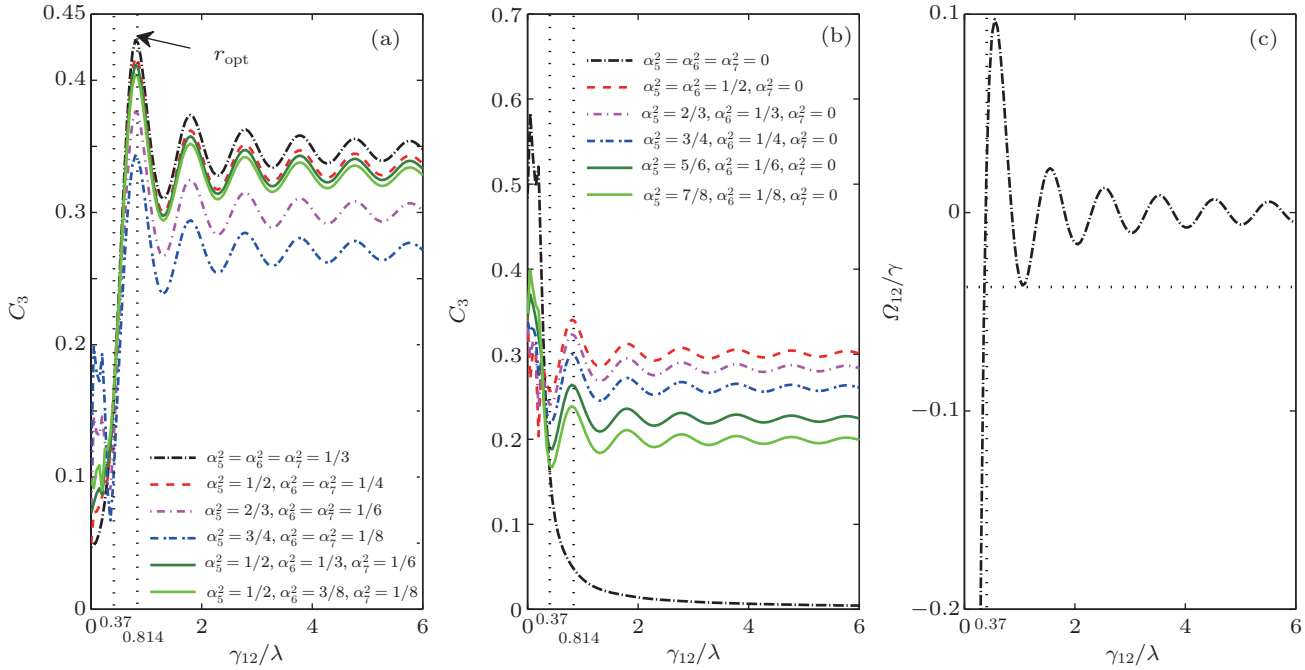


Fig. 3. (color online) The C_3 versus r_{12}/λ with $\gamma t = 1$ and (a) initially entangled states or (b) initially separable states. (c) The Ω_{12}/γ versus r_{12}/λ with $\theta = 5\pi/6$.

of the entanglement). So, with appropriate probabilities α_i, the long-term entanglement can obtain a large value. At relatively large distance r_{12} (i.e., $r_{12} > 0.37\lambda$), there will be a strong resemblance between the presence and absence of the dipole–dipole interaction, namely, the entanglement behaves as the exponential decay. With a further increase in distance r_{12} (i.e., $\gamma_{12} \ll \gamma$), the collective damping and the dipole–dipole interaction decay to zero (see Figs. 2(c) and 3(c)) and the dynamical behaviors of the entanglement behave as that of three independent atoms in a common environment.

For the initial entanglement, from Eq. (10), we can readily calculate

$$C_3^0(t=0) = \frac{2\sqrt{2}}{\sqrt{3}}\sqrt{\alpha_6^2\alpha_7^2 + \alpha_5^2\left(1-\alpha_5^2\right)}. \tag{15}$$

To estimate the difference between the initial entanglement (C_3^0) and the stationary entanglement (C_3^∞), we use Eqs. (14) and (15), and plot the entanglement versus α_5^2 for both initially entangled and separable states in Fig. 5(a). Note that C_3^0 (C_3^∞) behaves as a non-monotonic increasing (decreasing) function of α_5^2. In other words, in the course of increasing α_5^2, C_3^0 (C_3^∞) is first increasing (decreasing) too, but after reaching a maximum (minimum), it will be decreasing down to zero (increasing to a certain value equal to $(8/27)^{1/2}$). Furthermore, there is a competition between C_3^0 and C_3^∞. For the initially entangled (separable) states, C_3^0 exceeds C_3^∞ when $\alpha_5^2 \in [0, 0.949]$ ($\alpha_5^2 \in [0.069, 0.933]$), while C_3^∞ exceeds C_3^0 when $\alpha_5^2 \in [0.949, 1]$ ($\alpha_5^2 \in [0, 0.069]$ and $\alpha_5^2 \in [0.933, 1]$).

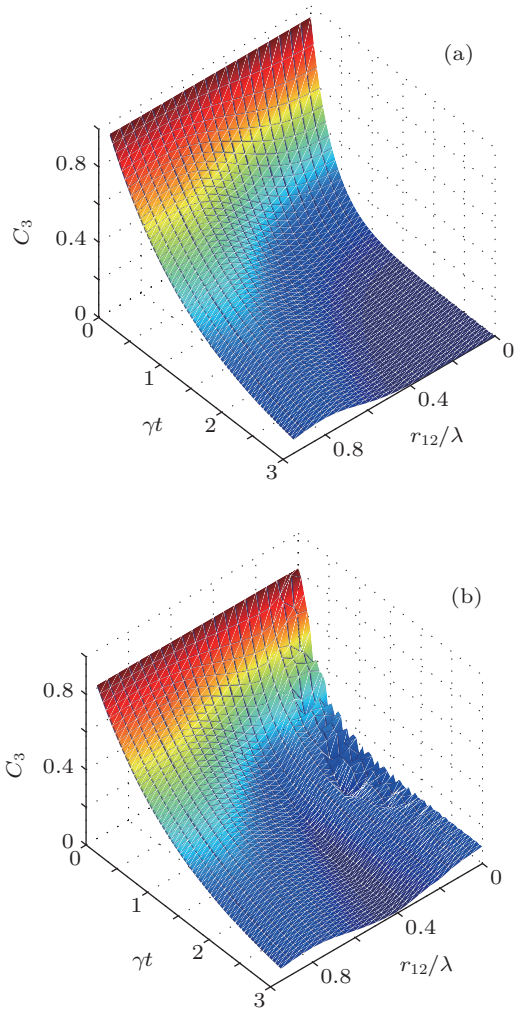


Fig. 4. (color online) A 3D view of C_3 versus r_{12}/λ and γt with (a) $\alpha_5 = \alpha_6 = \alpha_7 = 1/\sqrt{3}$ or (b) $\alpha_5 = 2/\sqrt{6}$, $\alpha_6 = \alpha_7 = 1/\sqrt{6}$.

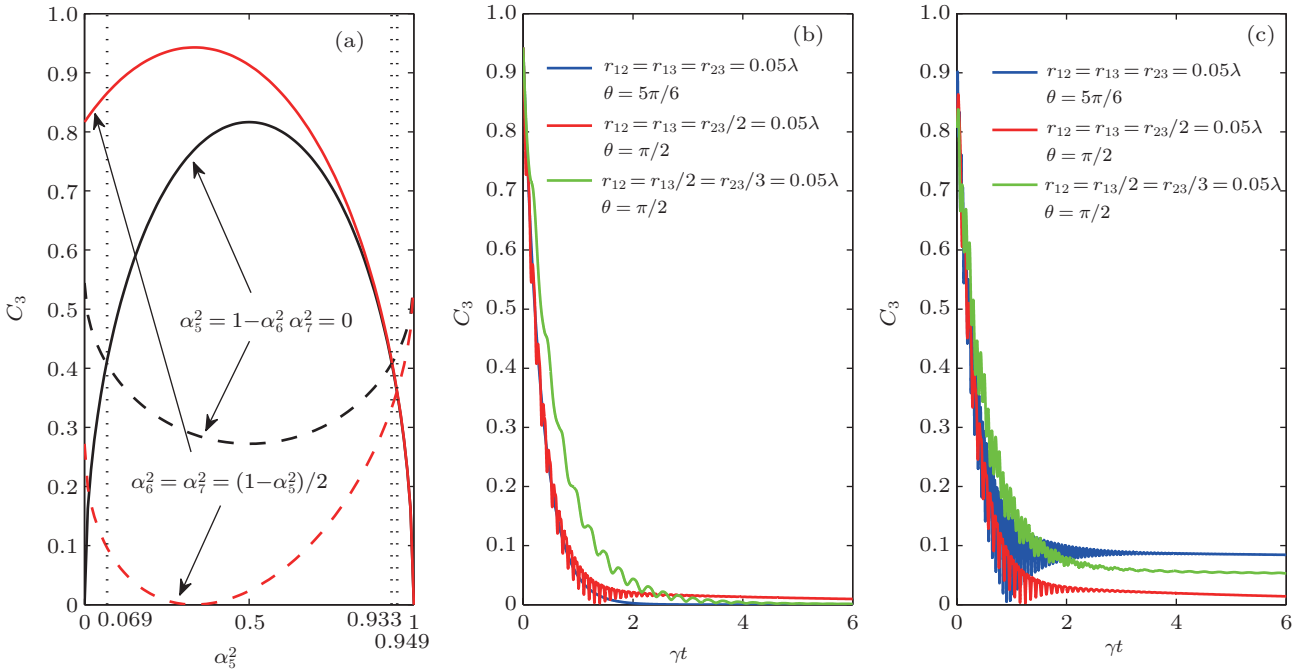


Fig. 5. (color online) (a) The C_3 versus α_5^2 for various initial conditions. The solid (red, black) line is for C_3^0, and the dashed (red, black) line is for C_3^∞. The C_3 versus γt for various values of r_{ij}/λ and (b) $\alpha_5 = \alpha_6 = \alpha_7 = 1/\sqrt{3}$ or (c) $\alpha_5 = 2/\sqrt{6}$, $\alpha_6 = \alpha_7 = 1/\sqrt{6}$.

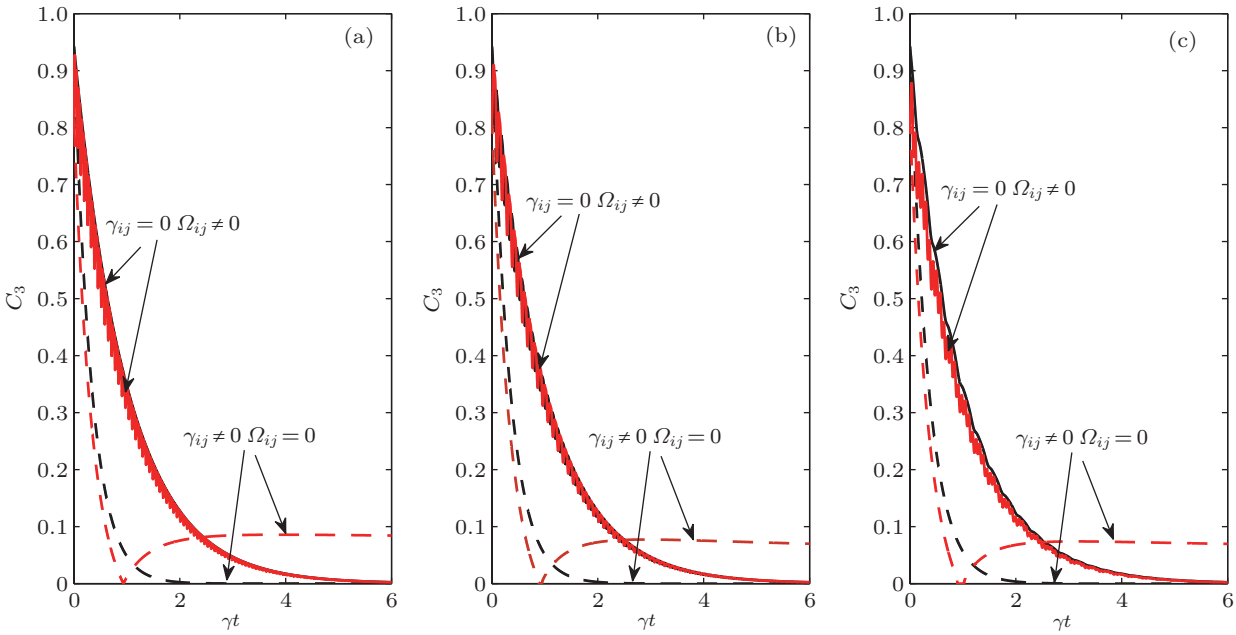


Fig. 6. (color online) The C_3 versus γt with (a) $r_{12}=r_{13}=r_{23}=0.05\lambda$, $\theta=5\pi/6$, (b) $r_{12}=r_{13}=r_{23}/2=0.05\lambda$, $\theta=\pi/2$, or (c) $r_{12}=r_{13}/2=r_{23}/3=0.05\lambda$, $\theta=\pi/2$. The black (solid, dashed) line is for $\alpha_5=\alpha_6=\alpha_7=1/\sqrt{3}$, and the red (solid, dashed) line is for $\alpha_5=2/\sqrt{6}$, $\alpha_6=\alpha_7=1/\sqrt{6}$.

Finally, we consider either case 2 or case 3 with $\theta=\pi/2$, namely, the atomic dipole moments are parallel to each other and are polarized in the direction perpendicular to the interatomic axis. When only two among r_{12}, r_{13}, r_{23} are equal (i.e., case 2) or when the r_{ij} are all different (i.e., case 3), as the analytical solutions of the density matrix elements are very complicated, only the numerical solutions can be used. The plots of C_3 for the three cases are shown in Figs. 5(b) and 5(c). For the interacting atoms, the entanglement of the three cases with different pairwise distances presents similar responses. More concretely, it is understandable that the entanglement can always be taken as being made up of the contributions of the collective damping and the dipole–dipole interaction associated with the interatomic distance. Thus, we respectively study the effects of the collective damping and the dipole–dipole interaction. From Fig. 6, we notice that when $\alpha_5=\alpha_6=\alpha_7=1/\sqrt{3}$, if there is the collective damping without the dipole–dipole interaction (i.e., $\gamma_{ij}\neq 0$ $(i\neq j)$ and $\Omega_{ij}=0$ $(i\neq j)$), the entanglement degrades exponentially with time. When $\alpha_5=2/\sqrt{6}$ and $\alpha_6=\alpha_7=1/\sqrt{6}$, the entanglement quickly decreases down to zero and then increases to a stationary value. On the other hand, if there is the dipole–dipole interaction without the collective damping (i.e., $\gamma_{ij}=0$ $(i\neq j)$ and $\Omega_{ij}\neq 0$ $(i\neq j)$), the entanglement exhibits damped oscillation, except when the probabilities α_i and the distances r_{ij} are all equal.

4. Conclusion

We have investigated the entanglement dynamics for a system composed of three atoms coupled with their common vacuum environment. If the interatomic distances are all equal, we can obtain the explicit solutions of the density matrix elements. There is an interesting feature in the system, an optimal distance emerges wherein the entanglement of the three atoms is at a maximum and the collective damping is at a minimum. For larger distances, the entanglement exhibits the exponential decay. For shorter distances, by adjusting the initial conditions, the oscillatory behavior of the short time entanglement occurs, whereas in the long time limit, the tripartite entanglement tends to a stationary value, and this provides a possible method for long time maintenance of the entanglement. If two among the three distances are equal or the distances are all different, the behavior of C_3 is similar to that of the cases with all equal distances.

Appendix A

The nonzero solutions of the density matrix elements $(\gamma_{12}=\gamma_{13}=\gamma_{23}, \Omega_{12}=\Omega_{13}=\Omega_{23})$ for the W states are

$$\begin{aligned}
\rho_{55} &= \frac{1}{9}[(2a_5-a_6-a_7)^2\mathrm{e}^{(\gamma_{12}-\gamma)t} \\
&\quad +(a_5+a_6+a_7)^2\mathrm{e}^{-(2\gamma_{12}+\gamma)t} \\
&\quad +(2a_5-a_6-a_7)(a_5+a_6+a_7)\mathrm{e}^{-\frac{1}{2}(\gamma_{12}+2\gamma+6\mathrm{i}\Omega_{12})t} \\
&\quad +(2a_5-a_6-a_7)(a_5+a_6+a_7)\mathrm{e}^{-\frac{1}{2}(\gamma_{12}+2\gamma-6\mathrm{i}\Omega_{12})t}], \\
\rho_{66} &= \frac{1}{9}[(a_5-2a_6+a_7)^2\mathrm{e}^{(\gamma_{12}-\gamma)t} \\
&\quad +(a_5+a_6+a_7)^2\mathrm{e}^{-(2\gamma_{12}+\gamma)t} \\
&\quad +(2a_6-a_5-a_7)(a_5+a_6+a_7)\mathrm{e}^{-\frac{1}{2}(\gamma_{12}+2\gamma+6\mathrm{i}\Omega_{12})t} \\
&\quad +(2a_6-a_5-a_7)(a_5+a_6+a_7)\mathrm{e}^{-\frac{1}{2}(\gamma_{12}+2\gamma-6\mathrm{i}\Omega_{12})t}],
\end{aligned}$$

$$
\begin{aligned}
\rho_{77} &= \frac{1}{9}[(a_5+a_6-2a_7)^2\,\mathrm{e}^{(\gamma_{12}-\gamma)t} \\
&\quad +(a_5+a_6+a_7)^2\,\mathrm{e}^{-(2\gamma_{12}+\gamma)t} \\
&\quad +(2a_7-a_5-a_6)(a_5+a_6+a_7)\,\mathrm{e}^{-\frac{1}{2}(\gamma_{12}+2\gamma+6\mathrm{i}\Omega_{12})t} \\
&\quad +(2a_7-a_5-a_6)(a_5+a_6+a_7)\,\mathrm{e}^{-\frac{1}{2}(\gamma_{12}+2\gamma-6\mathrm{i}\Omega_{12})t}], \\
\rho_{56} &= \frac{1}{9}[(-2a_5+a_6+a_7)(a_5-2a_6+a_7)\,\mathrm{e}^{(\gamma_{12}-\gamma)t} \\
&\quad +(a_5+a_6+a_7)^2\,\mathrm{e}^{-(2\gamma_{12}+\gamma)t} \\
&\quad -(a_5-2a_6+a_7)(a_5+a_6+a_7)\,\mathrm{e}^{-\frac{1}{2}(\gamma_{12}+2\gamma+6\mathrm{i}\Omega_{12})t} \\
&\quad +(2a_5-a_6-a_7)(a_5+a_6+a_7)\,\mathrm{e}^{-\frac{1}{2}(\gamma_{12}+2\gamma-6\mathrm{i}\Omega_{12})t}], \\
\rho_{57} &= \frac{1}{9}[(-2a_5+a_6+a_7)(a_5+a_6-2a_7)\,\mathrm{e}^{(\gamma_{12}-\gamma)t} \\
&\quad +(a_5+a_6+a_7)^2\,\mathrm{e}^{-(2\gamma_{12}+\gamma)t} \\
&\quad -(a_5+a_6-2a_7)(a_5+a_6+a_7)\,\mathrm{e}^{-\frac{1}{2}(\gamma_{12}+2\gamma+6\mathrm{i}\Omega_{12})t} \\
&\quad +(2a_5-a_6-a_7)(a_5+a_6+a_7)\,\mathrm{e}^{-\frac{1}{2}(\gamma_{12}+2\gamma-6\mathrm{i}\Omega_{12})t}], \\
\rho_{67} &= \frac{1}{9}[(a_5-2a_6+a_7)(a_5+a_6-2a_7)\,\mathrm{e}^{(\gamma_{12}-\gamma)t} \\
&\quad +(a_5+a_6+a_7)^2\,\mathrm{e}^{-(2\gamma_{12}+\gamma)t} \\
&\quad -(a_5+a_6-2a_7)(a_5+a_6+a_7)\,\mathrm{e}^{-\frac{1}{2}(\gamma_{12}+2\gamma+6\mathrm{i}\Omega_{12})t} \\
&\quad -(a_5-2a_6+a_7)(a_5+a_6+a_7)\,\mathrm{e}^{-\frac{1}{2}(\gamma_{12}+2\gamma-6\mathrm{i}\Omega_{12})t}], \\
\rho_{65} &= \rho_{56}^*, \quad \rho_{75}=\rho_{57}^*, \quad \rho_{76}=\rho_{67}^*, \\
\rho_{88} &= 1-\rho_{55}-\rho_{66}-\rho_{77}.
\end{aligned}
$$

References

[1] Yu T and Eberly J H 2004 *Phys. Rev. Lett.* **93** 140404
[2] Yu T and Eberly J H 2006 *Phys. Rev. Lett.* **97** 140403
[3] Ikram M, Li F L and Zubairy M S 2007 *Phys. Rev. A* **75** 062336
[4] Almeida M P, de Melo F, Hor-Meyll M, Salles A, Walborn S P, Souto Ribeiro P H and Davidovich L 2007 *Science* **316** 579
[5] Bellomo B, Lo Franco R and Compagno G 2007 *Phys. Rev. Lett.* **99** 160502
[6] Li Y, Zhou J and Guo H 2009 *Phys. Rev. A* **79** 012309
[7] Maniscalco S, Francica F, Zaffino R L, Gullo N L and Plastina F 2008 *Phys. Rev. Lett.* **100** 090503
[8] Wu Q and Zhang Z M 2014 *Chin. Phys. B* **23** 034203
[9] Shi J D, Wu T, Song X K and Ye L 2014 *Chin. Phys. B* **23** 020310
[10] López C E, Romero G, Lastra F, Solano E and Retamal J C 2008 *Phys. Rev. Lett.* **101** 080503
[11] Bellomo B, Lo Franco R and Compagno G 2008 *Phys. Rev. A* **77** 032342
[12] Lehmberg R H 1970 *Phys. Rev. A* **2** 883
[13] Tahira R, Ikram M and Zubairy M S 2011 *Opt. Commun.* **284** 3643
[14] Hu M L and Fan H 2012 *Ann. Phys.* **327** 851
[15] Ficek Z and Tana's R 2006 *Phys. Rev. A* **74** 024304
[16] Almutairi K, Tana's R and Ficek Z 2011 *Phys. Rev. A* **84** 013831
[17] Berrada K, Fanchini F F and Abdel-Khalek S 2012 *Phys. Rev. A* **85** 052315
[18] Nielsen M A and Chuang I L 2010 Cambridge University Press
[19] Mintert F, Carvalho A R R, Kuś M and Buchleitner A 2005 *Phys. Rep.* **415** 207
[20] Man Z X, Zhang Y J, Su F and Xia Y J 2010 *Eur. Phys. J. D* **58** 147
[21] Weinstein Y S 2010 *Phys. Rev. A* **82** 032326
[22] Siomau M and Fritzsche S 2010 *Eur. Phys. J. D* **60** 397
[23] Barredo D, Ravets S, Labuhn H, Béguin L, Vernier A, Nogrette F, Lahaye T and Browaeys A 2014 *Phys. Rev. Lett.* **112** 183002
[24] An N B, Kim J and Kim K 2010 *Phys. Rev. A* **82** 032316
[25] An N B, Kim J and Kim K 2011 *Phys. Rev. A* **84** 022329
[26] Li M, Fei S M and Wang Z X 2009 *J. Phys. A: Math. Theor.* **42** 145303
[27] Feng L J and Xia Y J 2015 *Acta Phys. Sin.* **64** 010302 (in Chinese)
[28] Sabín C and García-Alcaine G 2008 *Eur. Phys. J. D* **48** 435
[29] Acín A, Andrianov A, Costa L, Jané E, Latorre J I and Tarrach R 2000 *Phys. Rev. Lett.* **85** 1560